ingegneria sismica
International Journal of Earthquake Engineering
Anno XLIII - Num. 3 - 2026

FLUS method-based simulation of the effectiveness of Land utilization transformation on carbon pool dynamics under various future climatic conditions

Zhuoran Li[1], *Liwei Zhou*[1], *Yue Hu*[1], *Xixi Xu*[1] *and Shuhong Wu*[1,*]

[1] School of Ecology and Nature Conservation, Beijing Forestry University, Beijing, 100083, China

SUMMARY: *Land utilization transformation is a significant factor affecting regional carbon pool. As a representative city in the northern part of the province of Henan, Anyang City is facing the double pressure of urban development and ecological environment protection, and it is of vital importance to research the implications of Land utilization transformation on carbon pool for the sustainable development of the region. In this research, the implications of Land utilization transformation on carbon pool dynamics under various future climatic conditions in Anyang City were investigated on the basis of the FLUS method and the InVEST method. Three kinds of conditions of natural growth, eco-environmental conservation and arable land resource conservation were established to model and forecast the Land utilization transformation and carbon pool in 2030, taking the land utilization data between 2010 and 2020, fifteen driving factors are introduced as input indicators. The findings showed that the Kappa statistic of the FLUS method was 0.8152 and the OA accuracy was 0.8914, which suggested that the model simulation effect was satisfactory; in terms of Land utilization transformation, the intensity of Land utilization transformation in diverse conditions during 2020-2030 was in the following order: cultivated land conservation scenario > urban sprawl scenario > eco-environmental conservation scenario > natural growth scenario; in terms of carbon pool change, the land utilization transformation in 2010 was in the following order: cultivated land conservation scenario > urban sprawl scenario > eco-environmental conservation scenario > natural growth scenario. In terms of carbon pool dynamics, carbon pool exhibits an upward trend from 2010 to 2020, from 11.42 to 11.51. Among the future conditions, the eco-environmental conservation scenario shows the most significant increase in carbon pool, with the forest carbon pool increasing by 16.75% to 15,642.38 t and the grassland carbon pool increasing by 2.63% to 97,536.61 t. The research indicates that scientific planning of the land utilization structure and expanding forest coverage and grassland will have a beneficial impact on the enhancement of regional carbon pool and the promotion of ecological sustainable development.*

KEYWORDS: *Land utilization transformation; FLUS method; Carbon pool; Eco-environmental conservation; Scenario simulation; InVEST method*

1 Introduction

Global warming is a serious global environmental problem currently facing the world, which has a wide and profound impact on global ecological systems, human welfare and socio-

*lzhuor@126.com
https://doi.org/10.65102/is20261156 Published: 10 June, 2026

economic evolution [1, 2]. From the Industrial Revolution to the present, anthropogenic activities including forest loss, urban sprawl, and massive burning of fossil fuels have resulted in significant quantities of greenhouse gas (GHG) emissions, which have become the central cause driving global climatic warming [3-5]. And as the atmospheric CO2 concentration continues to increase, the research of the effect of Land utilization transformation on the dynamics of carbon pools under various future climatic conditions has turn into one of the central topics in global climatic warming research [6-8].

Land utilization transformation substantially influences the variations in vegetation and soil carbon pools, changing ecological structure and ecosystem services, and thus influencing the carbon biogeochemical cycle process of ecological systems [9, 10]. Terrestrial ecological systems, as a key component of the terrestrial surface, have a crucial impact on the global terrestrial carbon biogeochemical cycle, which is the basis for human survival and development, its carbon content sequestration function exerts a pivotal role in the global terrestrial carbon biogeochemical cycle and climatic warming [11-14]. Carbon pool dynamics in terrestrial ecological systems imply variations in biological carbon sequestration, altering CO2 levels in the air and affecting global climatic warming. Therefore, upgrading carbon pools in terrestrial ecological systems is a key means of reducing atmospheric CO2 concentration and mitigating global warming, as well as an effective way to achieve the goal of “carbon neutrality” [15-18]. Humans can enhance regulatory interventions in terrestrial ecological systems to improve their carbon sequestration capacity [19]. Therefore, it is important to explore the influences of land utilization transformation variations on ecosystem carbon pools to mitigate global climatic warming [20, 21]. To scientifically and reasonably regulate land utilization transformation and achieve the harmonious development of ecology and economy, this research is on the basis of the PLUS method to investigate the influences of land utilization transformation on the dynamics of carbon pools under various future climatic conditions [22-24]. As an emerging land utilization transformation simulation tool, the PLUS method is capable of simulate the land utilization transformation process in a spatially explicit manner by integrating natural and anthropogenic factors [25-27].

As anthropogenic global warming continues to intensify, the issue of carbon releases and stocks has attracted much attention. As an indispensable part of terrestrial ecological systems, land utilization and its change processes have a notable effect on the regional carbon biogeochemical cycle. Land utilization transformations change ecological structure and ecosystem services, which substantially influences the process of carbon pool capacity and release. In recent decades, China's fast-paced economic expansion and accelerated urban land expansion have resulted in drastic variations in land utilization structure, and these changes have caused dynamic Carbon pool dynamics. An accurate comprehension of the interrelationship between land utilization transformation and carbon pool is of considerable importance for the construction of regional carbon release mitigation and land resource management policies. As a representative city in the northern part of the province of Henan, Anyang City is located at the interface of Shanxi, Hebei and the province of Henans, and has a typical mild temperate continental seasonal climate, as well as a wide range of landscape types including mountains, hills and plains, which makes it an ideal area to research the interrelationship between land utilization transformation and carbon pool. In recent years, the fast-paced economic expansion of Anyang city is facing the double pressure of ecological environment protection and arable land resources protection. The research of the effectiveness of land utilization transformation on carbon pool in Anyang city can provide scientific basis for the construction of regional ecological civilization and the sustainable use of land resources. At present, scholars globally and nationally have carried out numerous studies on the interrelationship between land utilization transformation and carbon pool, mainly focusing on

the mechanism of land utilization transformation on carbon pool, the features of regional carbon pool dynamics and driving factors. However, due to regional variability and data acquisition limitations, there is a relative shortage of study on the effectiveness of land utilization transformation on carbon pool under various future climatic conditions in Anyang City. Land utilization simulation is an essential tool for anticipateing future land utilization patterns and researching carbon pool dynamics, and the FLUS (Future land utilization Simulation) model, which combines neural network and metacellular automata techniques, has high simulation accuracy and spatial and temporal continuity, and is capable of precisely characterize the process of land utilization transformation under complex conditions. Meanwhile, the Carbon stock simulation module of the InVEST method can simplify the carbon biogeochemical cycle process and estimate the regional carbon pool according to the terrestrial carbon density of different land utilization types, which provides an effective tool for the research of carbon pool dynamics.

In this research, Anyang city was chosen as the research area, and on the basis of the land utilization data between 2010 and 2020, three land utilization transformation conditions of natural growth, eco-environmental conservation and arable land resource conservation were constructed using the FLUS method with the integration of natural conditions and socio-economic contexts drivers to model and forecast the land utilization pattern of Anyang city in 2030. Then, the Carbon stock simulation module of the InVEST method was used to analyze the implications of land utilization transformations on carbon pools under diverse conditions. By comparing and analyzing the features of carbon pool dynamics under diverse conditions, the research explores the effect mechanism of land utilization restructuring on regional carbon pool, and provides scientific reference for the sustainable use of land resources and the execution of carbon neutral strategy in Anyang City. The specific research process is as follows: firstly, on the basis of multi-source remote sensing datasets, the land utilization data of Anyang city in 2010 and 2020 were obtained; secondly, 15 driving factors, such as elevation, slope, precipitation, etc., were collected; then, three land utilization conditions were constructed using the FLUS method, and the land utilization pattern of 2030 was simulated; lastly, on the basis of the InVEST method, the carbon pool was calculated in each time period, and the characteristics and impacts of carbon pool dynamics under the diverse conditions were analyzed. Finally, the carbon pool was calculated in each period on the basis of the InVEST method, and the characteristics and influencing factors of carbon pool dynamics under diverse conditions were analyzed. This research not only helps to understand the influence mechanism of Land utilization transformation on regional carbon pool, but also provides a scientific basis for land resource management and carbon release mitigation strategy formulation in Anyang City and similar regions.

2 Overview of the research area

Anyang is situated within the north of the province of Henan, at the interface of Shanxi, Hebei and the province of Henans, bordered by Changzhi in the west, Puyang in the east, Handan in the north, and Hebi and Xinxiang in the south, with a cumulative area of of 7413 km^2 .

The urban area of Anyang City is 1,218 km^2 , and the urban construction area of the central urban area is about 115 km^2 . It has one county administered city (Linzhou City), four subordinate counties (Anyang County, Shixian County, Neihuang County, and Tangyin County), and four city-administered districts (Wenfeng District, Beiguan District, Yindu District, and Long'an District).

The main canal is 66km long in Anyang City, passing through four administrative districts,

namely Tangyin County, Long'an District, Yindu District and Anyang County, and flowing through rivers such as the Tang River, the Yi River, the Anyang River and the Zhang River on the way. It enters Handan City of Hebei Province through Shijiahe Village of Anyang County. The main canal of the central line passes water mainly through the open channel, in addition, there are culverts, pipes, ferries and other facilities.

The place is situated within the northern mild temperate zone, continental seasonal climate. The four seasons change obviously, with sultry summer, chilly arid winter, and moderate spring and fall. The average temperature is 13.1℃~14.6℃. The city's average frost-free period is 189 days. The average precipitation of Anyang City in the past years is about 580~690mm, and the rainfall of the whole year is mainly in summer, with less rainfall in fall and winter, which is a dry period. The annual average relative humidity is 64%~69%. The total annual evaporation averages 1925~1993mm in all years, of which, summer is the most, fall is the second, and winter is the least. The wind direction in all seasons is mostly controlled by high-altitude airflow. In spring, summer and fall, the wind is mostly southerly, and in winter, the wind is mainly northerly.

The rivers in the area belong to the rainfall recharge type, and water level changes are influenced by seasonal and interannual variations in precipitation. The western mountainous area is a receiving water drainage area, receiving atmospheric precipitation and transferring it to replenish the underground, and the runoff from the surface river valleys is rare, making it a water-scarce area. Mountains to the west of the railroad in the hilly areas, in addition to receiving precipitation, there are groundwater outcrops, outpouring a stable amount, the formation of a number of rivers, and the underground dive complementary to the water supply is more guaranteed. The eastern plains, with low topography and high groundwater level, have sufficient water quantity to be a water-rich area, but the water quality is not as good as that in the west.

The surface topography is complex, with a wide range of landforms such as mountains, hills, plains and polders. The western part of the landform is dominated by the stripping tectonics, and the western part belongs to the hilly landform area. The area east of the railroad belongs to the range of low plains, the elevation is generally 72 meters, and gradually decreases to 50 meters to the east. The terrain is open and flat, with very little undulation, and can be called the pre-hill plain in terms of its surface form, which accounts for approximately 60% of the urban area.

The major vegetation categories are coniferous forests, broadleaf forests, thickets, swamps, cultivated vegetation, and grasslands. Among them, the cultivated vegetation is widely distributed, mainly biennial or biannual dry crops and deciduous fruit tree gardens, mainly in the central and southeastern regions. It is followed by scrub, mainly in the western mountainous regions.

3 Research methodology

3.1 Principles of the FLUS method

The FLUS method is adopted to simulate land utilization transformations and additionally to anticipate future land utilization. The model first uses artificial neural network method to determine the appropriateness probability of diverse types of land utilization in the research area on the basis of the Phase I land utilization data and driving factors (e.g., elevation, slope, precipitation, etc.). Then the sampling comparison method is adopted to calibrate and correct the first-phase land utilization data to guarantee the precision of the simulated results [28, 29].

During land utilization transformation simulation, the FLUS method introduces a self-

adaptive inertia competition strategy on the basis of roulette, which can be adopted to simulate various land utilization categories that change with natural and human behavior changes, thus effectively simulating the dynamic evolution of various land utilization types. Thanks to this mechanism, the FLUS method has high simulation accuracy, and its simulated results can be highly close to the actual land utilization distribution.

The FLUS method comprises two modules, namely, the module of appropriateness probability calculation on the basis of neural network and the module of metacellular automaton on the basis of adaptive inertia mechanism.

(1) Neural network-based appropriateness probability calculation module

Artificial neural network is an abstraction of the neural network of human brain, which is a kind of intelligent calculation designed after the internal neuron structure of human brain to achieve the optimization calculation of complex geographic system. It has powerful self-organization, self-learning and automatic control functions, so as to generate high probability suitability distributions and establish the deep interrelationship between the probability of occurrence of different land types and the driving factors. The BP-ANN in the FLUS method is a kind of multi-layer feed-forward neural network, whose structure contains an input layer, a hidden layer and an output layer. Specifically, the neurons in the input layer correspond to the driving factors of Land utilization transformation. While each neuron in the output layer is associated with a specific land utilization type. The setting of the hidden layer is determined on the basis of experience. By sampling from the distribution of single-period land utilization data, the model is capable of train and evaluate the probability of occurrence of each raster land utilization type, thus realizing accurate simulation and anticipateion of Land utilization transformations. The formula is:

$$p(p,k,t) = \sum w_{j,k} \times sigmoid(net_j(p,t)) \tag{1}$$

$$sigmoid(net_j(p,t)) = \frac{1}{1+e^{-net_j(p,t)}} \tag{2}$$

$$net_j(p,t) = \sum w_{i,j} \times x_i(p,t) \tag{3}$$

where $p(p,k,t)$ denotes the probability of land utilization type k on the raster p moment t. $w_{j,k}$ denotes the weights between the hidden and output layers. $sigmoid\left(net_j(p,t)\right)$ denotes the correlation function from the hidden layer to the output layer. $net_j(p,t)$ denotes the signal sent by the j th hidden layer to neuron j at t of grid p. $w_{i,j}$ denotes the signal between the input layer and the hidden layer. $x_i(p,t)$ the signal received by the i th input layer neuron at time t of grid p.

(2) Metacellular automata module on the basis of adaptive inertia principle

This module determines the transfer probability of Land utilization transformation by considering several factors, including the distribution probability of the neural network output, the neighborhood role, the conversion cost, and the adaptive inertia coefficient.

First, the neighborhood role. It reflects the influence of land utilization types around the image element on the central image element, i.e., the potential driving effect of neighboring land utilization types on the conversion of land utilization types in the central image element. The calculation formula is as follows:

$$\Omega_{p,k}^{t}=\frac{\sum_{N\times N} con\left(c_{p}^{t-1}=k\right)}{N\times N-1}\times w_{k} \tag{4}$$

where $\sum_{N\times N} con\left(c_{p}^{t-1}=k\right)$ denotes the total number of rasters occupied by k land utilization types at the end of $t-1$ under the $N\times N$ window. The w_k denotes the variable weights with different neighborhood action strengths between different land utilization types.

Second, the adaptive inertia coefficient. In the FLUS method, the inertia coefficients of each land utilization type are personalized on the basis of the difference between the current land utilization status and the target demand, and are adaptively adjusted in the iterative process. Taking forest land as an example, when the demand for forest land increases and the number of forest land decreases in the simulated results, the inertia coefficient of forest land will increase accordingly to curb the downward trend of the number of forest land and to motivate the conversion of other land utilization types to forest land. This mechanism helps to gradually adjust the number of land utilization types in the simulation process so that they converge to the preset target value. The specific calculation formula is as follows:

$$Interia_{k}^{t}=\begin{cases} Interia_{k}^{t-1} & if\ \left|D_{k}^{t-1}\right|\le\left|D_{k}^{t-2}\right| \\ Interia_{k}^{t-1}\times\dfrac{D_{k}^{t-2}}{D_{k}^{t-1}} & if\ D_{k}^{t-1}<\left|D_{k}^{t-2}\right|<0 \\ Interia_{k}^{t-1}\times\dfrac{D_{k}^{t-1}}{D_{k}^{t-2}} & if\ 0<D_{k}^{t-2}<D_{k}^{t-1} \end{cases} \tag{5}$$

where $Interia_{k}^{t}$ denotes the inertia coefficient of land utilization type k at t. D_{k}^{t-1}, D_{k}^{t-2} denote the difference between the demand and the number of rasters of the land utilization type k at the previous and the previous two iterations of the calculation, respectively.

Third, transformation cost. It is a key indicator to assess the difficulty of transforming the current land utilization type to other types. It reflects the potential barriers to conversion between different land utilization types. Under certain circumstances, when a land utilization type is prohibited to be converted to another type, the corresponding value in the conversion cost matrix will be set to 0. If conversion is allowed, the corresponding value will be set to 1.

Fourth, the total probability of land utilization transformation. This is derived by iterative computation through a metacellular automaton. This calculation process involves assigning each land utilization type to each raster to simulate the dynamic change of land utilization. The specific calculation formula is as follows:

$$TP_{p,k}^{t}=P_{p,k}\times\Omega_{p,k}^{t}\times Interia_{k}^{t}\times\left(1-SC_{c\to k}\right) \tag{6}$$

where $TP_{p,k}^{t}$ denotes the total probability that land utilization type k is at raster p at time t. $\Omega_{p,k}^{t}$ denotes the probability that land utilization type k occurs at raster p. $SC_{c\to k}$ denotes the transfer cost from land utilization type c to k. $1-SC_{c\to k}$ represents the difficulty level of transformation.

Fifth, land utilization transformation simulation. Simulate the transformation process between land utilization types and its competition with other types.

3.2 Parameter setting and program operation

(1) Neighborhood factor and weight

Neighborhood factor indicates the interaction between different land utilization types and between different land utilization units within the neighborhood, and its expression is:

$$\Omega_{p,k}^{t}=\frac{\sum_{N\times N} con\left(c_{p}^{t-1}=k\right)}{N\times N-1}\times\omega_{k} \tag{7}$$

where $\sum_{N\times N} con\left(c_{p}^{t-1}\right)$ denotes the total number of rasters of the k th land utilization type at the end of the last iteration in the neighborhood window of $N\times N$. The ω_k is the weight of the neighborhood role of each land utilization type. In this paper, we use 3×3 Moore's neighborhood, and the number of iterations is 500.

(2) Conversion cost matrix

The conversion cost matrix characterizes the difficulty of converting from the current land utilization type to the demand land utilization type. There are only two values 0 and 1 in the conversion cost matrix, this paper needs to set three conversion cost matrices for diverse conditions as shown in the analysis below.

3.3 Accuracy verification

Kappa statistic is a multivariate discrete method for evaluating the classification accuracy and error matrix of remote sensing images. This accuracy test method simultaneously considers various missed and misclassified image elements beyond the diagonal. For the accuracy test of the future land utilization anticipateion results of the FLUS method, it is achieved by the Validation module in the software, and the calculation formula is as follows:

$$k=\frac{p_0-p_e}{1-p_e} \tag{8}$$

$$p_0=\frac{\sum_{i=1}^{C}T_i}{n} \tag{9}$$

$$p_e=\frac{\sum_{i=1}^{C}a_i\times b_i}{n^2} \tag{10}$$

where p_0 is the overall classification accuracy, p_e is the intermediate process variable, C is the total number of land utilization type categories, here 7. T_i is the number of samples in each category that are correctly classified, a_i is the assumed number of true samples in each land utilization type category, and b_i is the anticipateed number of samples in each land utilization type category.

The simulation effects corresponding to different Kappa statistics are shown in Table 1.

Table 1: The analog effect of different Kappa statistics

Kappa statistic	0-0.2	0.2-0.4	0.4-0.6	0.6-0.8	0.8-1
Simulation effect	low	worse	medium	higher	height

3.4 InVEST method

The Carbon stock simulation module in the InVEST method was used to analyze the regional carbon pool and its dynamics [30].The Carbon stock simulation module simplifies the process of carbon cycling and determines the carbon densities of four carbon pools, above-ground biomass, below-ground biomass, organic matter in the soil, and dead organic matter, in each land utilization type according to different land utilization types. Then, the area of each land utilization type was multiplied by its corresponding average terrestrial carbon density, and finally summarized and summed up to arrive at the total carbon pool in the research area.

The terrestrial carbon density was calculated as:

$$C_i = C_{i-above} + C_{i-below} + C_{i-dead} + C_{i-soil} \tag{11}$$

where C_i is the terrestrial carbon density of the i th land category. $C_{i-above}$ is the terrestrial carbon density of above-ground organisms of the i th landrace. $C_{i-below}$ is the terrestrial carbon density of below-ground organisms of the i th landrace. C_{i-dead} is the terrestrial carbon density of dead organic matter for the i th landrace. C_{i-soil} is the terrestrial carbon density of soil organic matter of the i th landrace.

The carbon pool is calculated as:

$$C_{i-total} = C_i \times A_i \tag{12}$$

where $C_{i-total}$ is the total carbon pool of the i th land category in the region. C_i is the terrestrial carbon density of the i th land category, and A_i is the area of the i th land category.

4 Analysis of future land-use change and carbon pool projections

4.1 FLUS method setup

(1) Probability calculation on the basis of neural network

In the neural network training, add the 2010 land utilization data and 15 driving factors, set the number of hidden layers of the neural network to 12, and finally get the distribution probability data of various types of land. Among them, the training effect of grassland, cropland and forest land is better, and the training effect of water and permanent snow and ice is relatively poor.

(2) To test the simulation accuracy, with the help of the accuracy verification module of GeoSOS-FLUS, the simulated 2020 land-use data and the actual observed 2020 land-use data are used as the model input data, the confusion matrix is established, and the random sampling mode is selected with a sampling rate of 10% to carry out the verification of simulation accuracy.

The Kappa statistic, OA accuracy, and FoM index were calculated to be 0.8152, 0.8914, and 0.0315, respectively, indicating that the simulated land changes are highly similar to the observed land changes, and that the anticipateion of future conditions with the FLUS method is more reliable.

(3) Empirical parameter settings of the FLUS method

The parameters affecting the simulated results of the FLUS method are mainly the neighborhood weights, the amount of future pixels and the conversion rules. The empirical parameter settings of the model are given in the user manual of the future Land utilization

transformation scenario simulation model software.

In this paper, we firstly take the land utilization anticipateion in 2010 provided in the user manual and the relevant literature parameter settings in the place, and utilize the land utilization data in 2000 and 2020 to carry out the simulation of land utilization in 2030.

The meaning of the parameters and the specific way of setting them are:

a. Neighborhood weight of land characterizes the expansion capacity of a certain type of land utilization, the larger the neighborhood parameter is, the stronger the expansion capacity is, and the parameter ranges from 0~1. Different settings of the neighborhood weight parameter influences the simulation operation of the metacellular automata, and the size of the weight factor also influences the simulated results of the model.

The neighborhood parameters set by the user manual adopt the historical experience method, i.e., the parameters are set by past experience as well as relevant knowledge, and in this paper, the neighborhood weight parameters of each class are set separately.

b. The anticipateion of the future image metrics is achieved using the FLUS software coupled Markov model.

c. For the transfer matrix, the model developer refers to the manual to give the transfer matrix on the basis of historical experience and policy, such as limiting the conversion of arable land to forest land is prohibited, and water bodies are prohibited to be converted to other land, etc., i.e., the model parameter setting is somewhat subjective. In this paper, with reference to the relevant research and the actual situation of the place, the following limitations are adopted for the conversion of land categories: forest land and grassland can be converted to land categories except wetland and water body, cultivated land can be converted to all other land categories, snow and glacier can only be converted to itself and unutilized land, city and water body can not be changed, and the unutilized land can only be converted to the city and grassland in general, so that the transfer matrix of the land can be obtained.

4.2 Setting of land-use conditions

Considering the current development pattern of the site, the strategy of eco-environmental conservation and high-quality development, the execution of the project of farmland withdrawal to forests and grasslands, the basic farmland resource conservation system strictly implemented by the state, and the accelerated development of urban land expansion in the future, etc., the setup of multiple conditions is achieved by modifying the transfer probability matrix, the neighborhood factor, and the cost matrix, and the land-use demands, neighborhood factors, and cost matrices of the diverse conditions are shown below, respectively.

(1) Natural growth scenario

In this scenario, the Land utilization transformation still continues the trend of Land utilization transformation from 2010 to 2020, and no other conditions are set, and the land demand of the region in 2030 is estimated by Markov chain with a step of 10 years, and the cost matrix and neighborhood factor are consistent with the parameters of the 2020 land utilization simulation.

(2) Eco-environmental conservation scenario

In this scenario, the expansion of cropland and urban land slows down, and the growth of forest land and grassland accelerates. Firstly, it is set that the probability of transferring forest land, grassland and water to barren and urban areas decreases by 30%% and 60% respectively, and the probability of transferring cropland to forest land increases by 15%. Secondly, on the basis of the natural growth scenario, the neighbor parameter of barren and urban land category is reduced by 0.1, and the neighbor parameter of forest land, grassland and water area is increased by 0.1, and finally the land transfer level is set in the cost matrix as: forest land>grassland>water area>others.

(3) Cultivated land resource conservation scenario

This scenario mainly achieves the growth of arable land area by restricting the transfer of arable land to other land categories, and reduces the probability of transferring arable land to construction land by 55%, the probability of transferring arable land to forest land, grassland, and waters by 45%, and the probability of transferring arable land to unused land by 90% on the basis of natural growth. At the same time, adjusting the neighborhood factor of cropland on the basis of natural growth increases by 0.3, unused land decreases by 0.25, and the cost matrix restricts cropland from transferring to barren land categories.

The future land utilization demand (number of like elements) for diverse conditions is shown in Table 2.

It can be seen that under the ecological conservation scenario, the demand for watershed, woodland and grassland utilization is the highest and barrenness is reduced to 15193. Permanent snow and ice always remain the same size in all three conditions.

Table 2: Requirements for land utilization in diverse conditions in the future

Land demand	Natural growth situation	Eco-environmental conservation	Protection of cultivated land
Waters	4152	4231	4107
Woodland	70326	71529	69056
Grass	412436	413785	401019
Desolation	18969	15193	17554
Ploughing	254578	254132	27068
City	15565	13404	11927
Permanent ice	124	124	124

The future ELAS values for each category for diverse conditions are shown in Figure 1. In the eco-environmental conservation scenario, the ELAS values of watershed, forest land, and grassland are greater than those of the natural growth scenario and the cultivated land conservation scenario.

In the eco-environmental conservation scenario and the cultivated land conservation scenario, the barren land decreases, and the ELAS values are 0.56 and 0.54, respectively. Lower than the natural growth scenario.

In the cultivated land conservation scenario, urban land was the highest with an ELAS value of 0.95.

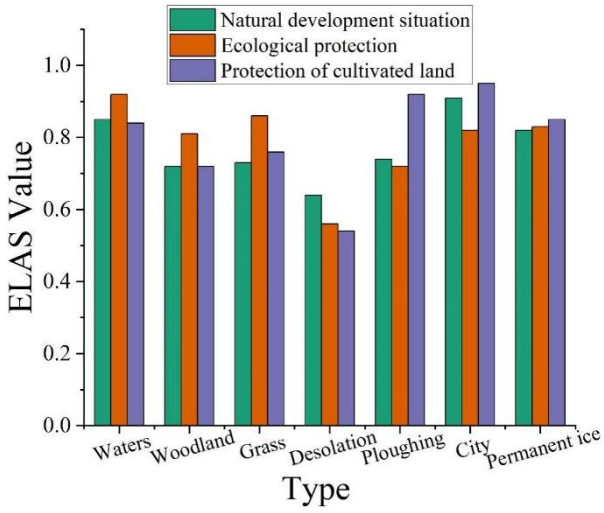

Figure 1: The ELAS value of classes in diverse conditions in the future

The land transfer cost matrix for diverse conditions is shown in Fig. 2, where a, b, c, d, e, f, and g denote watershed, forest land, grassland, barren, cropland, urban, and permanent snow and ice, respectively. Figures (a), (b), and (c) show the land transfer cost matrices under the natural growth scenario, eco-environmental conservation scenario, and cultivated land conservation scenario, respectively.

Overall, the FLUS method has high flexibility in scenario setting and can meet the regulations and development needs of different groups. In addition, the setting of diverse conditions in this paper mainly relies on subjective decision-making, but considering the non-stability of Land utilization transformation driven by socio-economic and anthropogenic decision-making, subjective analysis is still of considerable importance significance in the anticipateion of Land utilization transformation.

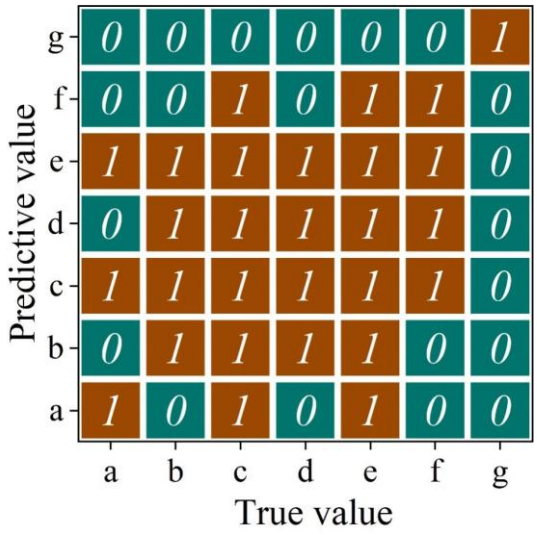

(a) Natural growth situation

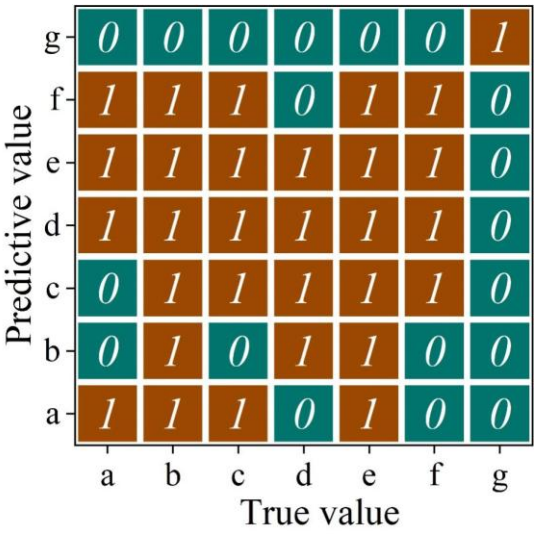

(b) Eco-environmental conservation

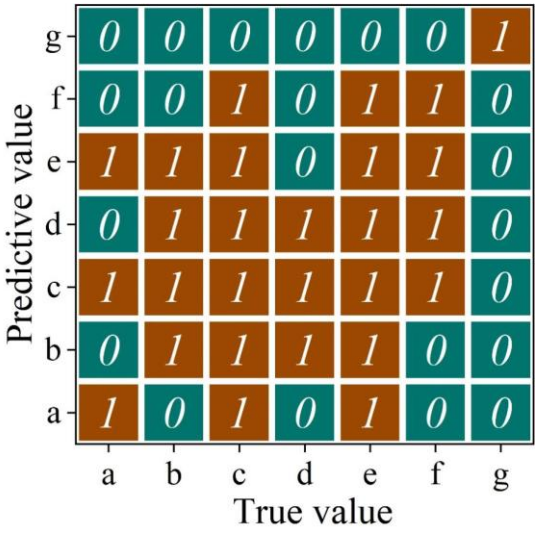

(c) Protection of cultivated land

Figure 2: Diverse conditions land transfer cost matrix

4.3 Spatial and temporal patterns of land-use change

The attitude of Land utilization transformation dynamics under various future conditions is shown in Table 3. In the table, a, b, c, d, e, f, and g denote waters, forest land, grassland, barren,

cropland, urban, and permanent snow and ice, respectively.

Analyzing the variations in the land categories in the research area, it was found that waters showed a balanced expansion in diverse conditions, with a relatively fast growth rate of 0.4251% in the eco-environmental conservation scenario. Woodland, grassland, cropland and barren are in equilibrium under diverse conditions, but woodland shows a decrease in size only under the cultivated land conservation scenario, at -0.0922%.

Grassland expands slowly only under the eco-environmental conservation scenario at 0.0896%. Cropland shows an increase in size only under the cultivated land conservation scenario and at a faster rate of 0.3456%. Barrenness shows a slow expansion under the natural growth scenario and a faster reduction in area under the eco-environmental conservation scenario.

In terms of the comprehensive motivation, the drasticness of Land utilization transformations in diverse conditions during 2020-2030 is in the following order: cultivated land conservation scenario > urban sprawl scenario > eco-environmental conservation scenario > natural growth scenario.

Table 3: In the future, diverse conditions are used to use change dynamics

Time period	Index	a	b	c	d	e	f	g
Natural growth situation	Single dynamic/%	0.2536	0.0715	-0.0077	0.0654	-0.0197	3.4251	-0.0658
	Spatial dynamic model /%	5.7580	2.3245	2.2365	5.5411	2.2694	13.0048	2.6394
	Trend and state index/%	0.0513	0.0448	-0.0028	0.0152	-0.0564	0.2758	-0.0255
	Integrated dynamic/%	0.0718						
Eco-environmental conservation	Single dynamic/%	0.4251	0.2043	0.0896	-0.8917	-0.2136	2.1423	-0.0667
	Spatial dynamic model /%	5.2698	3.4787	2.1243	4.7553	3.6695	12.2241	2.3345
	Trend and state index/%	0.0754	0.0663	0.0425	-0.2124	-0.0556	0.1824	-0.0296
	Integrated dynamic/%	0.0985						
Protection of cultivated land	Single dynamic/%	0.0365	-0.0922	-0.2153	-0.0643	0.3456	0.5263	-0.0524
	Spatial dynamic model /%	5.5635	1.7585	2.2353	5.3625	3.0121	11.2436	2.2453
	Trend and state index/%	0.0072	-0.0565	-0.1125	-0.0125	0.1243	0.0524	-0.0233
	Integrated dynamic/%	0.1124						

4.4 Analysis of carbon pool results

Land utilization data and terrestrial carbon density coefficients for different time periods were added to the carbon pool module of the InVEST method, and the carbon pool and terrestrial carbon density of the site in 2010, 2015, 2020 and 2030 under the three conditions were calculated.

The carbon pool and terrestrial carbon density of the site from 2010 to 2030 are shown in Figure 3. From The findings run out by the model, it can be seen that the carbon pool and terrestrial carbon density of the research area were $11.42\times10^{6}t$ and $31.89\,t/hm^{2}$ in 2010, and in 2015, the carbon pool and terrestrial carbon density were $11.46\times10^{6}t$ and $31.92\,t/hm^{2}$, an increase of $0.04\times10^{6}t$ and $0.03\,t/hm^{2}$, respectively, during the five-year period.2020 is 0.05 $\times10^{6}t$ and $0.02\,t/hm^{2}$, respectively, from 2015.

Generally speaking, carbon pools are on an rising trend in this period, mainly because the execution of the policy of farmland withdrawal to forests under this period has resulted in an rising trend within the scope of grassland and forest land.

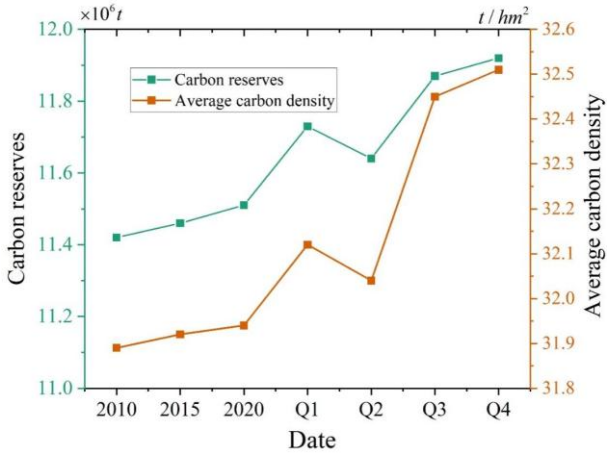

Figure 3: The carbon reserves and terrestrial carbon density of 20100~ 2030

4.5 Analysis of carbon pool dynamics by land-use type

Using the InVEST method, the carbon pool under diverse conditions for the site from 2010 to 2030 was obtained, and the findings obtained at different stages were subtracted in Arc GIS using a raster calculator to obtain the magnitude of change.

The variations in carbon pool of each land type at different stages are shown in Table 4.

From the perspective of land utilization types, cropland carbon pool under each scenario from 2015 to 2030, the fastest rate of decrease was from 2015 to 2020, with a rate of 2.36%, decreasing by 175,863.22 t. Overall, cropland carbon pool under each scenario from 2015 to 2020 and from 2020 to 2030 in the research area was decreasing, but cultivated land conservation scenario had the decline is the smallest. The carbon pool increased by 95,263.41t at a rate of 1.78% in 2010~2015, mainly because the area of cultivated land was increasing in that period.

Grassland carbon pool is increasing in diverse conditions from 2015 to 2030, and its fastest growth is from 2015 to 2020. In 2010~2015 carbon pool decreased at a rate of 2.37% by 71456.24 t. Overall, grassland carbon pool in the research area was increasing in all conditions from 2010~2030, but the largest increase in carbon pool was observed in the ecological security scenario.

Carbon pool in forest land showed an rising trend in all conditions from 2010 to 2030. And the carbon pool in the ecological security scenario increased the most, with a rate of 16.75% by 15,642.38 t. Overall, the reason for the growth in the whole period is due to the increase within the scope of forest land and the protection of the ecological environment.

Table 4: Different stages of carbon reserves in different stages

Ground class		Ploughing	Grass	Woodland	Construction land	Unexploited
2010-2015	Varying quantity	95263.41	-71456.24	2285.63	11985.26	-15316.21
	Amplitude	1.78	-2.37	2.45	22.01	-1.23
2015-2020	Varying quantity	-175863.22	156866.25	3215.36	7152.36	-1543.26
	Amplitude	-2.36	5.02	4.25	11.34	-0.23
Natural growth situation	Varying quantity	-5869.63	83585.32	942.36	15563.36	-12102.78
	Amplitude	-0.56	1.89	12.25	-1.24	-1.36
Protection of cultivated land	Varying quantity	-29363.21	63659.89	142.36	-852.64	-1548.36
	Amplitude	-0.53	1.93	12.14	-1.28	-0.19
Ecological safety situation	Varying quantity	-58593.63	97536.61	15642.38	13125.21	-14002.23
	Amplitude	-1.00	2.63	16.75	18.24	-1.45

5 Conclusion

On the basis of the FLUS method and InVEST method, this research analyzed the implications of Land utilization transformation on carbon pool in Anyang city under diverse conditions, and came to the following conclusions.

The FLUS method has a high simulation accuracy of Land utilization transformation in Anyang city, with a Kappa statistic of 0.8152 and an OA accuracy of 0.8914, indicating that the model is suitable for the simulation of Land utilization transformation in Anyang city. Among the three conditions, the drastic Land utilization transformations during the period of 2020-2030 were as follows: arable land resource conservation scenario > urban sprawl scenario > eco-environmental conservation scenario > natural growth scenario, and the combined motivation was 0.1124%, 0.0985% and 0.0718%, respectively.

From 2010 to 2020, the carbon pool of Anyang city exhibits an upward trend, from 11.42 to 11.51. Among the three future conditions, the ecological conservation scenario shows the most significant increase in carbon pools, mainly in the increase of carbon pools in forest land and grassland. Although the area of forest land is small, due to its high terrestrial carbon density per unit area, the carbon pool under the eco-environmental conservation scenario increases at a rate of 16.75%, which contributes significantly to the regional carbon pool.

Different land utilization types have different characteristics of carbon pool dynamics: cropland carbon pool shows an overall decreasing trend from 2010 to 2030, but the decreasing rate is the smallest under the cultivated land conservation scenario. The carbon pool in grassland exhibits an upward trend from 2015 to 2030, with the most significant increase under the eco-environmental conservation scenario. Carbon pools in forest land show an rising trend in all conditions, with growth rates ranging from 12.14% to 16.75%.

The research indicates that expanding forest coverage land and grassland has a beneficial impact on increasing the regional carbon pool, and the execution of eco-environmental conservation measures can effectively enhance the regional carbon sink function. It is recommended to strengthen the protection of ecological land in land-use planning, optimize the land-use structure, coordinate the interrelationship between economic development and eco-environmental conservation, and promote the sustainable development of the region.

References

[1] DARWIN, R. (2017). The Impact of Global Warming on Agriculture: A Ricardian. Climate Change, 125.

[2] Kweku, D. W., Bismark, O., Maxwell, A., Desmond, K. A., Danso, K. B., Oti-Mensah, E. A., ... & Adormaa, B. B. (2018). Greenhouse effect: greenhouse gases and their impact on global warming. Journal of Scientific research and reports, 17(6), 1-9.

[3] Mikhaylov, A., Moiseev, N., Aleshin, K., & Burkhardt, T. (2020). Global climate change and greenhouse effect. Entrepreneurship and Sustainability Issues, 7(4), 2897.

[4] Mohajan, H. K. (2017, March). Greenhouse gas emissions, global warming and climate change. In Proceedings of the 15th Chittagong Conference on Mathematical Physics, Jamal Nazrul Islam Research Centre for Mathematical and Physical Sciences (JNIRCMPS), Chittagong, Bangladesh (Vol. 16).

[5] Filonchyk, M., Peterson, M. P., Zhang, L., Hurynovich, V., & He, Y. (2024). Greenhouse

gases emissions and global climate change: Examining the influence of CO2, CH4, and N2O. Science of The Total Environment, 173359.

[6] Bréon, F. M., Broquet, G., Puygrenier, V., Chevallier, F., Xueref-Remy, I., Ramonet, M., ... & Ciais, P. (2015). An attempt at estimating Paris area CO 2 emissions from atmospheric concentration measurements. Atmospheric Chemistry and Physics, 15(4), 1707-1724.

[7] Wang, Z., Li, X., Mao, Y., Li, L., Wang, X., & Lin, Q. (2022). Dynamic simulation of land use change and assessment of carbon storage based on climate change scenarios at the city level: A case study of Bortala, China. Ecological Indicators, 134, 108499.

[8] Tian, L., Tao, Y., Fu, W., Li, T., Ren, F., & Li, M. (2022). Dynamic simulation of land use/cover change and assessment of forest ecosystem carbon storage under climate change scenarios in Guangdong Province, China. Remote Sensing, 14(10), 2330.

[9] Zhu, L., Song, R., Sun, S., Li, Y., & Hu, K. (2022). Land use/land cover change and its impact on ecosystem carbon storage in coastal areas of China from 1980 to 2050. Ecological Indicators, 142, 109178.

[10] Fu, Y., Huang, M., Gong, D., Lin, H., Fan, Y., & Du, W. (2023). Dynamic simulation and prediction of carbon storage based on land use/land cover change from 2000 to 2040: A case study of the Nanchang urban agglomeration. Remote Sensing, 15(19), 4645.

[11] Schimel, D., Pavlick, R., Fisher, J. B., Asner, G. P., Saatchi, S., Townsend, P., ... & Cox, P. (2015). Observing terrestrial ecosystems and the carbon cycle from space. Global Change Biology, 21(5), 1762-1776.

[12] Hari, M., & Tyagi, B. (2022). Terrestrial carbon cycle: tipping edge of climate change between the atmosphere and biosphere ecosystems. Environmental Science: Atmospheres, 2(5), 867-890.

[13] Luo, Y., Keenan, T. F., & Smith, M. (2015). Predictability of the terrestrial carbon cycle. Global change biology, 21(5), 1737-1751.

[14] Piao, S., Zhang, X., Chen, A., Liu, Q., Lian, X., Wang, X., ... & Wu, X. (2019). The impacts of climate extremes on the terrestrial carbon cycle: A review. Science China Earth Sciences, 62, 1551-1563.

[15] Lal, R., Smith, P., Jungkunst, H. F., Mitsch, W. J., Lehmann, J., Nair, P. R., ... & Ravindranath, N. H. (2018). The carbon sequestration potential of terrestrial ecosystems. Journal of soil and water conservation, 73(6), 145A-152A.

[16] Ni, J. (2013). Carbon storage in Chinese terrestrial ecosystems: approaching a more accurate estimate. Climatic Change, 119(3), 905-917.

[17] Singh, S. K., Thawale, P. R., Sharma, J. K., Gautam, R. K., Kundargi, G. P., & Juwarkar, A. A. (2015). Carbon sequestration in terrestrial ecosystems. Hydrogen production and remediation of carbon and pollutants, 99-131.

[18] Xu, L., Yu, G., He, N., Wang, Q., Gao, Y., Wen, D., ... & Ge, J. (2018). Carbon storage in China's terrestrial ecosystems: A synthesis. Scientific Reports, 8(1), 2806.

[19] Sharma, S., Jain, P. K., & Soloman, P. E. (2023). Carbon Storage Potential of Soil in Diverse Terrestrial Ecosystems. Nature Environment & Pollution Technology, 22(4).

[20] Hernández-Guzmán, R., Ruiz-Luna, A., & González, C. (2019). Assessing and modeling the impact of land use and changes in land cover related to carbon storage in a western basin in Mexico. Remote Sensing Applications: Society and Environment, 13, 318-327.

[21] Chang, X., Xing, Y., Wang, J., Yang, H., & Gong, W. (2022). Effects of land use and cover change (LUCC) on terrestrial carbon stocks in China between 2000 and 2018. Resources, Conservation and Recycling, 182, 106333.

[22] ZHAO, Z. H., XU, Z. R., CHENG, S. K., LU, C. X., & LIU, G. H. (2016). Analysis on dynamic of carbon storage in Tibet attributable to land use and land cover change. Journal of Natural Resources, 31(5), 755-766.

[23] Zhang, F., Zhan, J., Zhang, Q., Yao, L., & Liu, W. (2017). Impacts of land use/cover change on terrestrial carbon stocks in Uganda. Physics and Chemistry of the Earth, Parts A/B/C, 101, 195-203.

[24] Wei, Z., Ling, L., Wang, Q., & Luo, D. (2025). Multi-Scenario Land Use Change Dynamic Simulation and Carbon Stock Assessment of Man–Nature in Border Mountainous Areas. Sustainability, 17(4), 1695.

[25] Wu, Q., Wang, L., Wang, T., Ruan, Z., & Du, P. (2024). Spatial–temporal evolution analysis of multi-scenario land use and carbon storage based on PLUS-InVEST model: A case study in Dalian, China. Ecological Indicators, 166, 112448.

[26] Li, X., Li, C., Yu, S., Cheng, L., Li, D., Wang, J., & Zhao, H. (2024). Dynamic Simulation of Land Use Change and Assessment of Carbon Storage Based on the PLUS Model: A Case Study of the Most Livable City, Weihai, China. Sustainability, 16(24), 10826.

[27] Wang, Q., Zhang, W., Xia, J., Ou, D., Tian, Z., & Gao, X. (2024). Multi-Scenario Simulation of Land-Use/Land-Cover Changes and Carbon Storage Prediction Coupled with the SD-PLUS-InVEST Model: A Case Study of the Tuojiang River Basin, China. Land, 13(9), 1518.

[28] Zuopeng Zhang,Zhe Li & Zhirong Li. (2025). Evaluating the change and trend of construction land in Changsha City based GeoSOS-FLUS model and machine learning methods. Scientific Reports,15(1),9602-9602.

[29] Jinlin Lai, Shi Qi, Jiadong Chen, Jianchao Guo, Hui Wu & Yizhuang Chen. (2025). Exploring the spatiotemporal variation of carbon storage on Hainan Island and its driving factors: Insights from InVEST, FLUS models, and machine learning. Ecological Indicators, 172, 113236-113236.

[30] Jinxia Zhang,Zhao Liu,Zilong Guan,Lixia Wang,Jiaqi Zhang & Zhongqing Han. (2025). Balancing future urban development and carbon sequestration: A multi-scenario InVEST model analysis of China's urban clusters. Journal of environmental management, 380, 125003.